Division accuracy in a stochastic model of Min oscillations in *Escherichia coli*

Rex A. Kerr*†‡, Herbert Levine†§, Terrence J. Sejnowski*†¶‖, and Wouter-Jan Rappel†§

*Computational Neurobiology Laboratory and ‖Howard Hughes Medical Institute, The Salk Institute for Biological Studies, La Jolla, CA 92037; and †Center for Theoretical Biological Physics, §Department of Physics, ¶Division of Biological Sciences, University of California, San Diego, La Jolla, CA 92093

Edited by Harry L. Swinney, University of Texas, Austin, TX, and approved November 7, 2005 (received for review July 11, 2005)

Accurate cell division in *Escherichia coli* requires the Min proteins MinC, MinD, and MinE as well as the presence of nucleoids. MinD and MinE exhibit spatial oscillations, moving from pole to pole of the bacterium, resulting in an average MinD concentration that is low at the center of the cell and high at the poles. This concentration minimum is thought to signal the site of cell division. Deterministic models of the Min oscillations reproduce many observed features of the system, including the concentration minimum of MinD. However, there are only a few thousand Min proteins in a bacterium, so stochastic effects are likely to play an important role. Here, we show that Monte Carlo simulations with a large number of proteins agree well with the results from a deterministic treatment of the equations. The location of minimum local MinD concentration is too variable to account for cell division accuracy in wild-type, but is consistent with the accuracy of cell division in cells without nucleoids. This finding confirms the need to include additional mechanisms, such as reciprocal interactions with the cell division ring or positioning of the nucleoids, to explain wild-type accuracy.

dynamics | MCELL | FtsZ

The rod-shaped bacterium *Escherichia coli* reproduces by elongating along its long axis, duplicating its genetic material, and dividing symmetrically into two daughter cells. Wild-type *E. coli* locates the plane of cell division at 0.5 ± 0.013 of the distance along the long axis of the cell (1). This accuracy is surprising given that the cell apparently relies on the collective action of individual molecules that are a few nanometers long to measure the center of a cell that is a few microns long.

A variety of proteins are known to be involved in cell division in *E. coli*. In particular, cell division is implemented mechanically by a contractile ring formed predominantly by the FtsZ protein (2); the location of the FtsZ ring determines the site of cell division. During cell division, the bacterial chromosomes for the daughter cells are collected into two nucleoids that segregate to either side of the cell (3, 4) and fill much of the interior of the cell. Formation of the FtsZ ring is inhibited by the presence of the nucleoids (1, 5), leaving three bands in which to place the FtsZ ring: either pole or the center. The Min proteins are required for selection of the central band and precise positioning within the central band (1). MinC inhibits formation of the FtsZ ring, whereas MinD appears to recruit MinC (reviewed in ref. 6). These proteins show dynamic changes in localization throughout the cell (7–9). In particular, MinD oscillates from end to end of the cell with a period of ≈40 s (7); averaged over many cycles, MinD is at a higher concentration at the ends of the cell than in the center. Another protein, MinE, forms moving bands inside the cell and is required for MinD oscillations (10, 11). Thus, dynamic oscillations of MinD and MinE set up a concentration minimum of MinD at the center of the cell, leading to a low concentration of MinC at the center and enabling FtsZ ring formation at the cell's midpoint but not at its poles (12). Of the two mechanisms required for accurate cell division, the Min system seems more important: in mutants missing MinC, MinD, and MinE, placement of the plane of cell division is not restricted to three tightly defined nucleoid-free regions, but rather is broadly distributed (1). In nucleoid-free cells, the division apparatus still assembles near the center of the cell, but with a reduced accuracy of ±0.062 rather than ±0.013 cell lengths (1, 5).

Because of the importance of the Min system and the unexpected dynamics of the proteins, a variety of models of Min oscillations have been developed by using deterministic (13–18) or stochastic methods (19). These models reproduce many of the features of the biological system, including a concentration minimum of MinD at the center of the cell. Deterministic models of Min oscillations assume that there are a sufficiently large number of proteins to treat their concentrations as continuous variables. However, there are only a few thousand Min proteins in an *E. coli* cell (20, 21). If MinD proteins were stationary, the cell would have to position the FtsZ ring on the basis of only tens of Min molecules locally. Oscillations provide an opportunity for the cell to take multiple independent samples of Min concentration, but it is not immediately apparent whether this temporal averaging is sufficient to allow accurate midpoint determination. Therefore, we asked whether, in the context of current models, the observed accuracy of cell division could be achieved by simply selecting the site at which the local MinD concentration is lowest.

To answer this question, we constructed a stochastic simulation of Min oscillations based on the reaction–diffusion scheme of Huang *et al.* (16, 22). This scheme was an attractive choice for three reasons. First, a deterministic analysis of the scheme reproduces many features of the biological oscillations quite well. Second, the scheme is based in biologically realistic interactions. Third, the scheme is of a form that is immediately suitable for simulation in the stochastic modeling program MCELL (23, 24). Using MCELL, we reproduced the results of the deterministic analysis for a large number of molecules and demonstrated robust oscillations that can be disrupted by decreasing the number of Min proteins in the cell. In addition, we have examined the accuracy with which the cell could determine its midpoint if it made its decision based solely on finding the minimum local MinD concentration. The scheme can account for the accuracy of cells without nucleoids, but fails to reproduce the accuracy of wild-type cells.

Methods

Monte Carlo Modeling of Min Oscillations. MCELL is a Monte Carlo modeling program for cellular microphysiology. It has been described in detail elsewhere (23) and has been validated extensively. In brief, it represents cell membranes and other boundaries as arbitrary triangulated surfaces specified by the user, and represents each molecule as a point diffusing within

Conflict of interest statement: No conflicts declared.

This paper was submitted directly (Track II) to the PNAS office.

Abbreviations: D/E, MinD/MinE ratio; CV, coefficient of variation.

‡To whom correspondence should be addressed. E-mail: kerr@salk.edu.

those boundaries. Each molecule diffuses stochastically by picking a distance and direction of motion consistent with diffusion of a point source over some short time step, and travels in a straight line to reach that endpoint. A moving molecule reflects when its path intersects an impermeable surface element, and reacts stochastically when its path of motion intersects another molecule. The probability of each reaction is set by specifying a bulk rate constant, which is then internally converted into the appropriate probability of reaction per collision. A stochastic MCELL model consists of a series of chemical reactions specifying the rates of reaction, the diffusion constants for the diffusing molecular species, and a model geometry. We used a new version of MCELL that allows variable-length time steps; for our models of Min oscillations, this reduced the run time of the simulations by an order of magnitude.

The Huang *et al.* scheme (16) uses a series of chemical reactions (illustrated in Fig. 1*A*)

$$\mathrm{MinD_{ADP}} \xrightarrow{k_1} \mathrm{MinD_{ATP}}$$

$$\mathrm{MinD_{ATP}} + (m) \xrightarrow{k_2} \mathrm{MinD(m)}$$

$$\mathrm{MinD_{ATP}} + \mathrm{MinD(m)} \xrightarrow{k_3} 2\mathrm{MinD(m)}$$

$$\mathrm{MinD_{ATP}} + \mathrm{MinDE(m)} \xrightarrow{k_3} \mathrm{MinDE(m)} + \mathrm{MinD(m)}$$

$$\mathrm{MinE} + \mathrm{MinD(m)} \xrightarrow{k_4} \mathrm{MinDE(m)}$$

$$\mathrm{MinDE(m)} \xrightarrow{k_5} \mathrm{MinD_{ADP}} + \mathrm{MinE}.$$

Here, (m) alone refers to a patch of membrane without anything bound to it, and (m) after the name of a molecular species indicates that the molecule is bound to the membrane. This series of chemical reactions, in contrast to the systems of equations used in other Min system models (13–15), is immediately suitable for simulation using MCELL. Each patch of membrane can be occupied by at most one molecule, so the self-aggregation reactions with rate k_3 require searching for a free patch of membrane for the new MinD(m) molecule. Because the deterministic equations do not include a term for depletion of binding sites, we used a fairly large value for the search radius (50–100 nm). Moderate changes to this value did not significantly change our results (data not shown). The values used for the reaction rates are given in Table 1. In the default simulations with 5,400 proteins, there were 4,000 membrane-binding sites per μm^2. The diffusion constants for $\mathrm{MinD_{ADP}}$, $\mathrm{MinD_{ATP}}$, and MinE were 2.5 $\mu m^2/s$. Membrane-bound molecules were not allowed to diffuse.

Model Geometry. We created a simple 20-sided polyhedral cylinder of 4-μm length with a 0.5-μm radius, as shown in Fig. 1*B*. For computational efficiency, we also created a model geometry consisting of a 4-μm-long rectangular box with sides of length $\sqrt{\pi}/2$, preserving the volume of the model cell, and decreased the rate constant k_2 for the side walls by a factor of $\sqrt{\pi}/2$ to account for the increased surface area and hence increased number of binding sites. By default, the model was populated with 5,400 molecules, as in ref. 16, with varying ratios of MinD to MinE. Initially, all MinE molecules were placed along the central axis 0.25 μm from one pole of the cell, and all MinD molecules were placed in ADP-bound form 0.25 μm from the opposite pole. To compare simulation results with experimental results, we ran all simulations for 20 min of simulated time

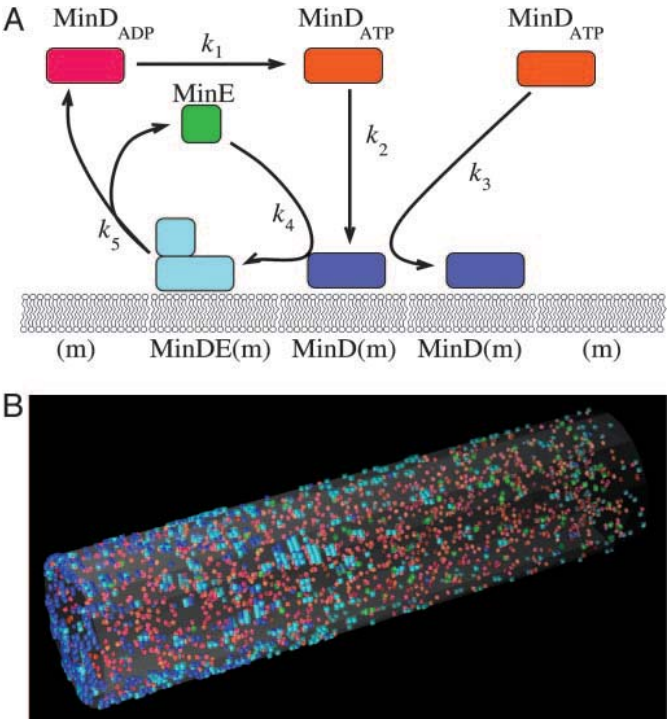

Fig. 1. Reactions and geometry of the stochastic Min oscillation model. (*A*) Reaction cycle. Cytosolic MinD in its ADP-bound form converts to an ATP-bound form with rate k_1. MinD-ATP binds to the membrane alone with rate k_2, and membrane-bound MinD (with or without MinE) catalyzes its own addition to the membrane at rate k_3. Cytosolic MinD binds membrane-bound MinD with rate k_4. Finally, the MinE/MinD complex dephosphorylates and dissociates into cytosolic MinE and MinD-ADP at rate k_5. (*B*) Snapshot of a simulation running inside a 4-μm-long, 0.5-μm-radius triangulated cylinder (transparent surface) after 3 min of simulated time. Each colored dot is a single molecule. Colors for each state are from *A*. There are 5,400 proteins and a MinD/MinE ratio of 4.0.

(approximately one cell division cycle in exponential growth phase); this represents the maximum time a cell has to measure MinD concentrations. We did not change the cell length during the simulation.

Deterministic Modeling of Min Oscillations. To compare the results from our stochastic simulations with deterministic solutions of the reaction scheme, we numerically integrated the equations of ref. 16, along with its parameter values, using a simple explicit time-stepping routine. Space was discretized by using a cubic (for the box geometry) or cylindrical (for the cylinder) grid with a grid spacing of 0.05–0.1 μm. We verified that a smaller grid spacing did not change the results appreciably (data not shown).

Measurement of Concentration and Oscillation Period. The local concentrations of Min proteins were determined by dividing the model cell into $n_b = 800$ bins of equal width along its long axis. The number of proteins in each bin was converted into a concentration, with a concentration of 2.7 μM corresponding to

Table 1. Reaction rates for the stochastic Min model in cylindrical geometry

Variable	k_1	k_2	k_3	k_4	k_5
Value	1.0	3.8×10^4	9.0×10^5	5.6×10^7	0.7
Units	s^{-1}	$M^{-1} \cdot s^{-1}$	$M^{-1} \cdot s^{-1}$	$M^{-1} \cdot s^{-1}$	s^{-1}

one molecule per bin. Concentrations were measured every $\delta_t = 0.1$ s. We verified that using $\delta_t = 0.2$ s gave equivalent results.

To quantify the fluctuations in the oscillation period, we defined the instantaneous oscillation period $T_{osc}(t)$ as the period that gave maximal correlation between MinE concentration profiles before and after t. For details, see *Supporting Text*, which is published as supporting information on the PNAS web site. We then computed the mean oscillation period $\bar{T}_{osc}$ by taking the mean of the instantaneous oscillation period over the ≈14 min of the trace for which it was defined [20 min, minus 180 s to allow any initial transients to subside, minus ≈200 s used as a window in the computation of $T_{osc}(t)$]. Similarly, we quantified the variability by computing the standard deviation of the instantaneous oscillation period.

Variable Stochasticity with Constant Dynamics. A bimolecular reaction of the form $A + B \rightarrow C$ can be written as a differential equation $\dot{C} = k \times A \times B$, where capital letters denote the concentration of the corresponding molecule. Increasing the concentrations by a factor of α yields $\alpha\dot{C} = \alpha^2 k \times A \times B$. Replacing k with k/α recovers the original equation and the original time course. Therefore, to run a simulation with N proteins instead of 5,400 while preserving the original dynamics, we replaced k_3 and k_4 with $k_3 \times 5{,}400/N$ and $k_4 \times 5{,}400/N$, respectively. The number of binding sites was also increased by $N/5{,}400$ to preserve the fractional depletion of binding sites, and k_2 was replaced by $k_2 \times 5{,}400/N$.

Estimation of Maximum Accuracy. To estimate the accuracy of cell division generated by picking local MinD concentration, we first divided the cell into 800 bins (5 nm per bin) and computed the membrane-bound MinD concentration in each bin. We then averaged the concentration in each bin over the lifetime of the cell (20 min) and applied a Gaussian blur of varying widths σ to represent the distance over which MinD can influence FtsZ ring formation. The bin with the lowest value was considered to be the local MinD-defined division site. To parameterize the accuracy, we computed the rms of the distances between the local MinD-defined division site on each trial and the midpoint of the cell.

For the default case (5,400 proteins, MinD/MinE = 4.0), we obtained the distribution of MinD-defined minima by performing 82 separate 20-min long simulations (results shown in Fig. 4*D*). Because each simulation takes ≈5 h on a 2.4-GHz AMD Opteron processor, this method was computationally too costly to allow a systematic exploration of parameter space. Therefore, we mimicked the concentration profiles by fitting a fourth-order polynomial to concentration profiles obtained from simulations, and then generating noise about that polynomial with the same power spectrum as found in the simulation. For details, see *Supporting Text*. To estimate the distribution of MinD-defined minima, we generated 1,000 mimicked concentration profiles based on five simulations and computed the positions of the minimums as described above. For the default case, the mean estimated distribution was 10–15% tighter than the distribution produced from 82 separate simulations. Therefore, this method leads to a slight overestimate of the accuracy of the local MinD-defined division site.

Results

Comparison Between Stochastic and Deterministic Model. A stochastic model of MinD and MinE oscillations was constructed following the deterministic set of reactions of Huang *et al.* (16), summarized in Fig. 1. To verify that the stochastic simulations could faithfully reproduce the deterministic results, we plotted the MinE concentration along the long axis of cell as a function of time and used this to compare the results from three different simulations: a stochastic simulation of the reactions in a cylindrical cell 1 μm in diameter and 4 μm long (shown in Fig. 1*B*), a stochastic simulation of the reactions in a rectangular cell of the same length and matched volume and surface reaction rates, and a deterministic simulation in a rectangular cell that directly implements the equations from ref. 16. As shown in Fig. 2*A*, all three simulations gave qualitatively similar results for the parameters we chose initially (the same as in ref. 16, except with a MinD/MinE ratio of 4.0).

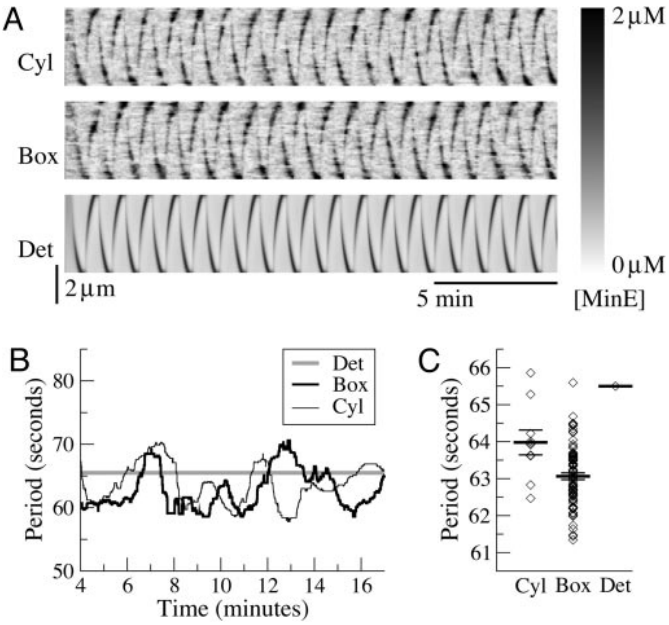

Fig. 2. Validation of the stochastic simulations. (*A*) Qualitative agreement between models. MinE concentration along the long axis of the cell (vertical axis) is plotted over time (horizontal axis). MinE moves from pole to pole of the cell in the stochastic simulations with cylindrical geometry (Cyl). Similar patterns are seen in a stochastic simulation run in a box (Box) and in a deterministic solution in a box (Det). (*B*) Stochastic fluctuations in oscillation period. The instantaneous oscillation periods for the cylindrical (thin line), box (thick line), and deterministic models (gray line) are shown. The data are from *A*. (*C*) Quantitative agreement between models. Oscillation periods are shown (diamonds) along with the means (large bars) and standard errors (small bars) for three simulations: cylindrical ($n = 10$ different random number streams), box ($n = 82$), and deterministic box.

MinE waves in the cylindrical and box stochastic models (Fig. 2*A*) were accompanied by noise with two related components. First, the concentration fluctuated from time point to time point, as expected from any model with a finite number of discrete particles. Second, the period of the oscillation fluctuated from cycle to cycle, as determined by observing the time between successive waves of MinE reaching one end of the cell. To quantify these fluctuations, we computed the instantaneous oscillation period over time (Fig. 2*B*) by measuring the time between maximally correlated MinE concentration profiles (see *Methods* and *Supporting Text*).

To test whether the results differed quantitatively between cylindrical and rectangular geometry, we ran the stochastic simulations several times using different random number streams ($n = 82$ for the rectangular box, $n = 10$ for the cylinder) and calculated the average oscillation period. The average period was 64.0 s for the cylinder and 63.1 s for the box, a statistically significant but minor difference ($P < 0.01$, Mann–Whitney rank-sum test). Because simulations using the box require less computation, we used that model for our subsequent analysis. We also verified that a model cell with rounded endcaps displayed similar quantitative results (data not shown).

To assess the accuracy with which the stochastic simulations

reproduce the deterministic result, we compared the stochastic and deterministic treatment of the box model. The period for the deterministic solution is 65.4 s, a modest but statistically significant increase ($P < 0.001$, t test) over the value from the stochastic simulations. This difference may be caused by the lack of discrete membrane binding sites in the deterministic solution; in the stochastic model, the cooperative interactions create clusters of membrane-bound MinD with all nearby binding sites depleted, whereas in the deterministic solution, membrane concentration varies smoothly and without limit.

Stochastic Disruption of Oscillations. To explore the effects of stochasticity in our model, we adjusted the protein number without altering the expected deterministic dynamics (see *Methods*). The number of proteins was varied from 10,800 down to 540 (Fig. 3*A*). The varying levels of stochasticity manifested in two ways. First, the local fluctuations in concentration from time point to time point became more apparent as the number of proteins was decreased (visualized as increasing "snow" in the concentration plots). Second, the oscillations ceased to be reliable for models with less than ≈1,500 proteins, although transient oscillatory behavior could still be observed (Fig. 3*A*).

We also varied the MinD/MinE ratio (hereafter D/E), which sets the oscillation period, to assess whether the magnitude of stochastic effects varied with period. As D/E was reduced to the minimal value that has a deterministic solution, the stochastic simulations became more sensitive to the number of proteins. To quantify the disruption of oscillations by noise we calculated the coefficient of variation (CV) of the oscillation period. Because unstable oscillations have a highly variable (and often ill-defined) oscillation period, the CV can be used to quantify the stability of oscillations.

With large numbers of proteins and high values of D/E, oscillations were stable and displayed a CV of ≈0.05, regardless of protein number or D/E ratio (Fig. 3*B*). Decreasing protein number eventually caused instability, with greater instability displayed for the fastest oscillations (low D/E ratio). Although a D/E value of 2.7 has a dynamic deterministic solution, we did not observe oscillations in any of the stochastic simulations at that value. Thus, in contrast to ref. 19, stochastic effects appear to dampen rather than drive oscillations in this model. We then examined the oscillation period of stable oscillations (specifically, oscillations with CV < 0.15). Within this region of stability, the oscillation period did not depend on the number of proteins and showed good agreement with the deterministic solution (Fig. 3*C*).

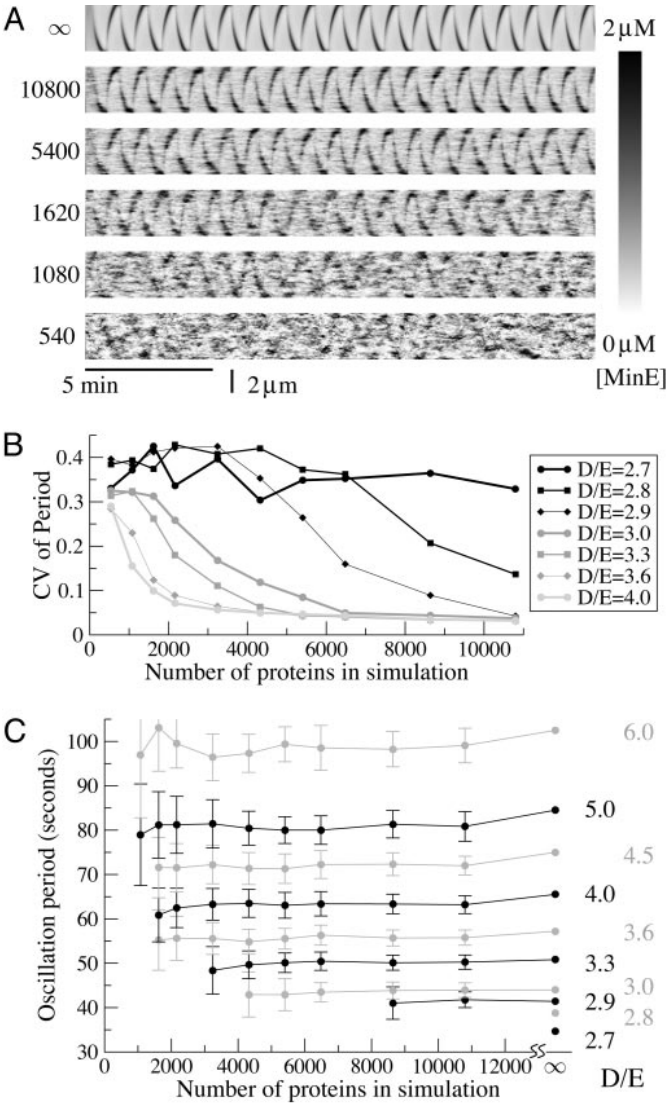

Fig. 3. Stochastic effects on oscillation period. (*A*) Oscillations are disrupted by decreasing protein number. MinE waves are plotted for the deterministic case (∞) and for stochastic models with decreasing numbers of proteins (indicated on left). In all cases, the total MinD/MinE ratio is D/E = 4.0, and the reaction rates have been altered to match the deterministic case (see *Methods*). (*B*) Rapid transition from stable to unstable oscillations. The coefficient of variation of the period of oscillation was determined for D/E ranging from 2.7 to 4.0, and protein numbers ranging from 540 to 10,800. Stable oscillations produce a low coefficient of variation in the period. The deterministic model has no dynamic solution for D/E ≤ 2.6. (*C*) Dependence of oscillation period on MinD/MinE. Shown is the mean oscillation period for a range of D/E values (indicated on right) and protein number (horizontal axis). Error bars indicate standard deviation of the period. Only stable oscillations are shown (CV < 0.15 from *B*).

Accuracy of Midpoint Determination. The key event in determining the accuracy of cell division is the placement of the FtsZ ring. Unfortunately, the mechanism of interaction between the Min proteins and the FtsZ proteins is not understood in much detail, and save for ref. 13, the localization of FtsZ has not been part of deterministic models. Thus, we did not directly incorporate FtsZ ring formation in our model. However, it is known that membrane-bound MinD recruits MinC, and MinC inhibits FtsZ ring formation. Therefore, we tested the following hypothesis: the cell only uses local interactions and chooses the position of the FtsZ ring based solely on the local MinD concentration. If this hypothesis is correct, then the position at which local MinD concentration is a minimum should define the center of the cell, and the accuracy of this positioning would represent an upper bound on the accuracy the cell can achieve. Because the precise duration over which MinD concentration is averaged is not known, we averaged for a full cell division cycle of 20 min.

We first plotted the membrane-bound MinD concentration along the length of the cell averaged over 20 min of oscillations with 5,400 proteins and D/E = 4.0 (black line in Fig. 4*A*). The shape of the profile was very nearly quadratic with a minimum at the cell center. To determine the depth of this minimum, we compared the central membrane-bound MinD concentration with the mean concentration (Fig. 4*B*). Both deterministic and stochastic simulations showed central minima that varied with D/E, but the stochastic simulation had a deeper minimum with parameters that gave stable oscillations. As before, the difference between the two curves is most likely due to the existence of discrete binding sites in our stochastic simulations.

The distance over which MinD can affect the FtsZ ring is not known. Therefore, we picked cell division sites by selecting the minimum membrane-bound MinD concentration after smooth-

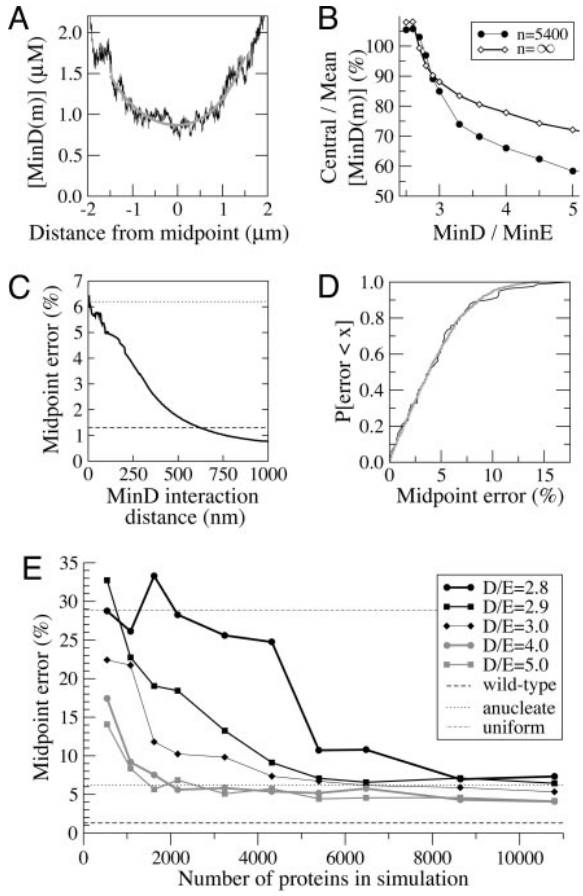

Fig. 4. Midpoint determination accuracy. (*A*) Membrane-bound MinD averaged over 20 min of oscillations in a rectangular box with MinD/MinE = 4.0 and 5,400 proteins. Average MinD concentration (black line) can be approximated as a fourth-order polynomial (gray line). (*B*) Depth of MinD concentration minimum at true midpoint of cell, measured as central value divided by mean value. The central value was taken from the polynomial fit to the stochastic data. (*C*) Accuracy of MinD minimum. Interaction distances were approximated as a Gaussian blur of the concentration profile, and the position of minimum MinD was measured on each smoothed profile. Midpoint error (solid line) is the mean rms distance between the true midpoint and the MinD minimum, measured as a fraction of cell length. Experimentally determined errors (from ref. 1) for wild-type (dashed line) and anucleate cells (dotted line) are included for reference. (*D*) Distribution of errors. Cumulative probability distribution of the midpoint error is shown for 82 full simulations (black line) and for 1,000 mimicked data sets (gray line) generated from 5 of the 82 simulations. The interaction distance was set to 50 nm. (*E*) Comparison with experimental data. A total of 1,000 mimicked data sets were generated from five simulations for each value of the parameters shown. Shown is the rms distance between the true cell midpoint and the MinD minima in the mimicked data sets.

ing with a Gaussian blur of various widths to approximate different interaction distances (Fig. 4*C*). A width of $\sigma = 500$–750 nm was needed to produce accuracy comparable to wild-type (0.013 cell lengths as reported in ref. 1, or a midpoint error of 1.3%; $n = 82$ simulations). Both the time scale (18 min) and spatial scale (≈ 1 μm) are surprising for local interactions with filaments with a lifetime of 8 s (25, 26) and a width of tens of nanometers. If we restricted the interaction distance to the size of a typical macromolecular complex ($\sigma \leq 50$ nm), accuracy decreased to $\approx$6%, similar to the value of 6.2% observed in cells without nuclei (1).

Although our model does not include nucleoid exclusion mechanisms, we wondered whether a different choice of parameters could reduce the midpoint error in the model without having to assume long-range interactions between MinD and FtsZ. To reduce the computation required, we devised a method to mimic concentration profiles by replicating the noise observed in five simulations; this gave good agreement with the distribution of errors found from running a full set of 82 simulations (Fig. 4*D*; $\sigma = 50$ nm). We then computed midpoint errors over a range of parameters (Fig. 4*E*). An accuracy of 4–7% was observed when either D/E ratios were high or the number of proteins was large; low D/E ratios coupled with small numbers of proteins led to division sites generated at uniformly at random. Once stable oscillations had been attained, increasing D/E or protein number only caused a slight improvement in accuracy, and accuracy stayed in the 4–7% range. Therefore, although the local MinD concentration cannot directly determine the cell midpoint to wild-type accuracy in our model, it can robustly account for the accuracy in the absence of nucleoids.

Discussion

Stochastic Effects on Min Oscillations. Our results show that the oscillation period in the stochastic simulations depends only weakly on the number of proteins and approaches the deterministic solution if the number of particles is large. However, if this number is below a critical value, oscillations fail. As shown in Fig. 3*C*, this value depends on the MinD/MinE ratio. A direct comparison of this value with experiments is difficult. Shih *et al.* (21) measured 2,000 MinD proteins and 1,400 MinE monomers (700 functional dimers) per cell. These values correspond to a model with 2,700 proteins and a MinD/MinE ratio of 2.85, a set of parameters that does not produce stable oscillations with our model, at least not with the rates taken from ref. 16. However, if the proteins are maintained at constant concentration, a 4-μm-long cell about to undergo cell division would have approximately twice that number (5,400 total, as in ref. 16), bringing the system closer to stability. To perform a more accurate comparison, it would be helpful to estimate the number of proteins in an individual cell and then run simulations with the same number of proteins in the same geometry.

Our model predicts that the depth of the minimum of average MinD at the center of the cell would be relatively constant except for parameters that were close to the limit for supporting oscillations. Furthermore, our results show that a very pronounced minimum in MinD concentration is unlikely. Fluorescence microscopy has revealed a MinD profile similar to what our model predicts (17), although for total MinD, not membrane-bound MinD. Further quantitative microscopy should help test the predictions of this model.

Midpoint Determination. Two poorly understood mechanisms work together to ensure an accurate cell division: nucleoid occlusion and the Min signaling system. In particular, the details of the nucleoid occlusion mechanism remain elusive, although it has been suggested that it is only responsible for restricting the possible division site to three regions (middle and poles), whereas the Min system is the main determinant of the midpoint determination. However, our results indicate that a simple scheme of determining the location for cell division by selecting the minimum MinD concentration in a local area, averaged over a cell's lifetime, is not sufficiently accurate to reproduce biological results. Because selecting a minimum in MinD concentration is also a difficult problem for the cell that could be affected by additional stochasticity in the selection mechanism, the results presented here should be viewed strictly as a lower bound on the error.

It is possible, of course, that refinements within the reaction scheme of the Min signaling system could improve the accuracy. For example, MinD forms long polymeric chains in bacteria (27, 28); in the model, MinD tends to cluster in unstructured rafts. The polymerization of MinD may impose geometrical con-

straints that are not captured by the simple model of MinD recruitment used here. For example, a model of MinD coils that alternately grow from opposite ends of the cell, as suggested in ref. 28, might result in a markedly steeper dip in MinD concentration, allowing greater accuracy. Alternatively, the interaction between MinD and the FtsZ ring may not be one-way. Models incorporating mutual antagonism between FtsZ ring formation and MinD coil formation may lead to a central FtsZ ring that is pushed from side to side by each wave of MinD, but which also prevents MinD from crossing. The nucleoids could then simply be responsible for starting the FtsZ ring in a reasonable range. Interaction dynamics such as these, if they exist, may be visible experimentally in bacteria expressing cyan and yellow fluorescent protein-labeled MinD and FtsZ.

Another possibility is motivated by noticing that the simulated reaction scheme we used for the Min signaling system is consistent with experiments that show that anucleated cells, obviously lacking the occlusion mechanism, display a greatly reduced cell division accuracy (1, 5). In fact, over a wide range of model parameters, the division accuracy obtained in our stochastic simulations is comparable to the accuracy obtained in these experiments (see Fig. 4*D*). This finding suggests that our model may capture the essential stochastic features of the Min system but needs to be expanded with a description of the nucleoid occlusion mechanism.

How might this nucleoid occlusion mechanism function? Our results indicate that this mechanism should not merely restrict the possible FtsZ ring formation sites but should be actively involved in midpoint determination. Further evidence for such an active role comes from experiments showing that cells missing the Min proteins have abnormally localized nucleoids (29). Perhaps the Min system has a twofold effect on cell division accuracy: a direct effect on FtsZ localization, transduced by MinC and based on local MinD concentration; and an indirect effect where MinD concentration acts to properly structure and position the nucleoids over a relatively long integration time, and nucleoid exclusion refines the position of the FtsZ ring. This model is appealing because it suggests a physical mechanism for averaging MinD concentration over a large fraction of the cell, which, as we have shown, can improve accuracy to the needed level.

We thank Dr. Thomas Bartol, Jr., for assistance with and advice on computational methods for stochastic modeling and 3D visualization of data. This work was supported by the National Science Foundation Physics Frontier Center-sponsored Center for Theoretical Biological Physics (Grants PHY-0216576 and PHY-0225630). Additional support was provided by National Institutes of Health Grant T32 0007220 (to R.A.K.) and the Howard Hughes Medical Institute (T.J.S.).

1. Yu, X.-C. & Margolin, W. (1999) *Mol. Microbiol.* **32,** 315–326.
2. Lutkenhaus, J. (1993) *Mol. Microbiol.* **9,** 403–409.
3. Valkenburg, J. A. C., Woldringh, C. L., Brakenhoff, G. J., van der Voort, H. T. M. & Nanninga, N. (1985) *J. Bacteriol.* **161,** 478–483.
4. Zimmerman, S. B. (2002) *J. Struct. Biol.* **142,** 256–265.
5. Sun, Q., Yu, X.-C. & Margolin, W. (1998) *Mol. Microbiol.* **29,** 491–503.
6. Lutkenhaus, J. (2002) *Curr. Opin. Microbiol.* **5,** 548–552.
7. Raskin, D. M. & de Boer, P. A. J. (1999) *Proc. Natl. Acad. Sci. USA* **96,** 4971–4976.
8. Hu, Z. & Lutkenhaus, J. (1999) *Mol. Microbiol.* **34,** 82–90.
9. Raskin, D. M. & de Boer, P. A. J. (1999) *J. Bacteriol.* **181,** 6419–6424.
10. Fu, X., Shih, Y.-L., Zhang, Y. & Rothfield, L. I. (2001) *Proc. Natl. Acad. Sci. USA* **98,** 980–985.
11. Hale, C. A., Meinhardt, H. & de Boer, P. A. J. (2001) *EMBO J.* **20,** 1563–1572.
12. Margolin, W. (2001) *Curr. Biol.* **11,** R395–R398.
13. Meinhardt, H. & de Boer, P. A. J. (2001) *Proc. Natl. Acad. Sci. USA* **98,** 14202–14207.
14. Howard, M., Rutenberg, A. D. & de Vet, S. (2001) *Phys. Rev. Lett.* **87,** 278102.
15. Kruse, K. (2002) *Biophys. J.* **82,** 618–627.
16. Huang, K. C., Meir, Y. & Wingreen, N. S. (2003) *Proc. Natl. Acad. Sci. USA* **100,** 12724–12728.
17. Meacci, G. & Kruse, K. (2005) *Phys. Biol.* **2,** 89–97.
18. Drew, D. A., Osborn, M. J. & Rothfield, L. I. (2005) *Proc. Natl. Acad. Sci. USA* **102,** 6114–6118.
19. Howard, M. & Rutenberg, A. D. (2003) *Phys. Rev. Lett.* **90,** 128102.
20. Zhao, C.-R., de Boer, P. A. & Rothfield, L. I. (1995) *Proc. Natl. Acad. Sci. USA* **92,** 4313–4317.
21. Shih, Y.-L., Fu, X., King, G. F., Le, T. & Rothfield, L. (2002) *EMBO J.* **21,** 3347–3357.
22. Kulkarni, R. V., Huang, K. C., Kloster, M. & Wingreen, N. S. (2004) *Phys. Rev. Lett.* **93,** 228103.
23. Stiles, J. R. & Bartol, T. M. (2001) in *Computational Neurobiology: Realistic Modeling for Experimentalists*, ed. de Schutter, E. (CRC Press, Boca Raton, FL), pp. 87–127.
24. Coggan, J. S., Bartol, T. M., Esquenazi, E., Stiles, J. R., Lamont, S., Martone, M. E., Berg, D. K., Ellisman, M. H. & Sejnowski, T. J. (2005) *Science* **309,** 446–451.
25. Anderson, D. E., Guieros-Filho, F. J. & Erikson, H. P. (2004) *J. Bacteriol.* **186,** 5775–5781.
26. Chen, Y. & Erickson, H. P. (2005) *J. Biol. Chem.* **280,** 22549–22554.
27. Suefuji, K., Valluzzi, R. & RayChaudhuri, D. (2002) *Proc. Natl. Acad. Sci. USA* **99,** 16776–16781.
28. Shih, Y.-L., Le, T. & Rothfield, L. (2003) *Proc. Natl. Acad. Sci. USA* **100,** 7865–7870.
29. Åkerlund, T., Gullbrand, B. & Nordström, K. (2002) *Microbiology* **148,** 3213–3222.